Electronic Supplementary Material (ESI) for Journal of Materials Chemistry

Evidence of non-stoichiometry effects in nanometric manganite perovskites : influence on the magnetic ordering temperature

Romain Epherre,[a] Cinta Pepin,[a] Nicolas Penin,[a] Etienne Duguet,[a] Stéphane Mornet,[a] Emil Pollert[b] and Graziella Goglio*[a]

Supplementary data

Table S1 : Structural parameters and reliability factors deduced from Rietveld refinement of XRD patterns for $La_{1-x}Sr_xMnO_{3+\delta}$ with x =0, 0.10, 0.20, 0.35 and 0.40. Occupancies were fixed with respect of chemical compositions (deduced from ICP and redox titration experiments).

$x_{théo}$		0	0.1	0.2	0.35	0.4
a (Å)		5.508(1)	5.507(1)	5.504(1)	5.488(2)	5.477(2)
c (Å)		13.342(3)	13.351(2)	13.366(2)	13.375(4)	13.381(9)
V (Å^3)		350.5(1)	350.1(1)	350.7(1)	348.8(2)	347.6(3)
La/Sr	Wyckoff site	***6a*** (0, 0, ¼)				
	Occ.	0.99	0.86 / 0.10	0.78 / 0.19	0.64 / 0.35	0.59 / 0.40
	B_{iso} (Å²)	0.35(9)	0.22(8)	0.07(6)	0.02(8)	0.00(8)
Mn	Wyckoff site	***6b*** (0, 0, 0)				
	Occ.	0.94	0.96	0.97	0.99	0.99
	B_{iso} (Å²)	1.0				
O	Wyckoff site	***18e*** (x, 0, ¼)				
	x	0.458(5)	0.458(3)	0.461(4)	0.467(4)	0.476(5)
	Occ.	1.0				
	B_{iso} (Å²)	1.0				
cRp (%)		22.3	16.0	14.6	18.5	17.6
cRwp (%)		15.5	13.6	12.5	13.1	12.7
R_{exp} (%)		12.4	10.4	10.1	11.1	11.5
R_{Bragg} (%)		8.7	7.7	6.1	6.7	5.6
χ^2		1.59	1.74	1.54	1.38	1.22

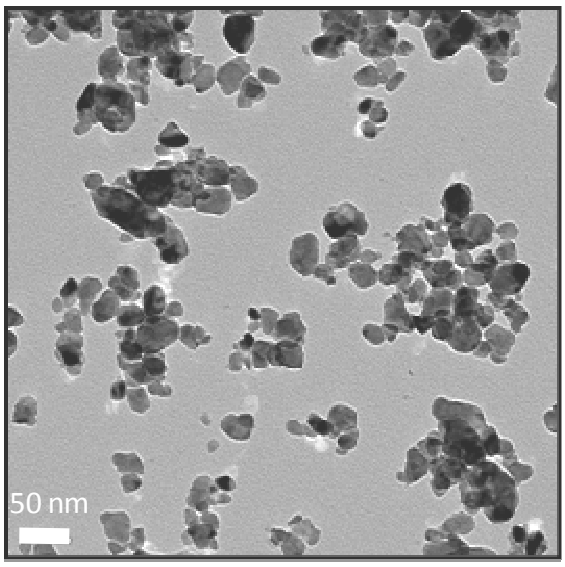

Figure S1 : TEM image of unaggregated manganite nanoparticles (x=0.18)

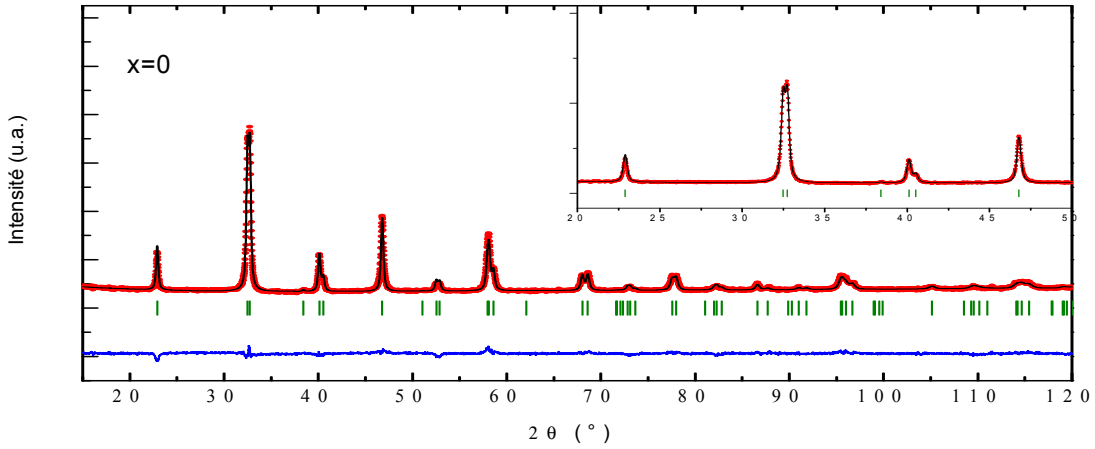

Figure S2 : Observed (red dots), calculated (black solid line), and difference (bottom, blue) X-ray powder diffraction patterns for $La_{1-x}Sr_xMnO_{3+\delta}$ with x = 0. A zoom in the 20-50° theta range is presented in the inset.

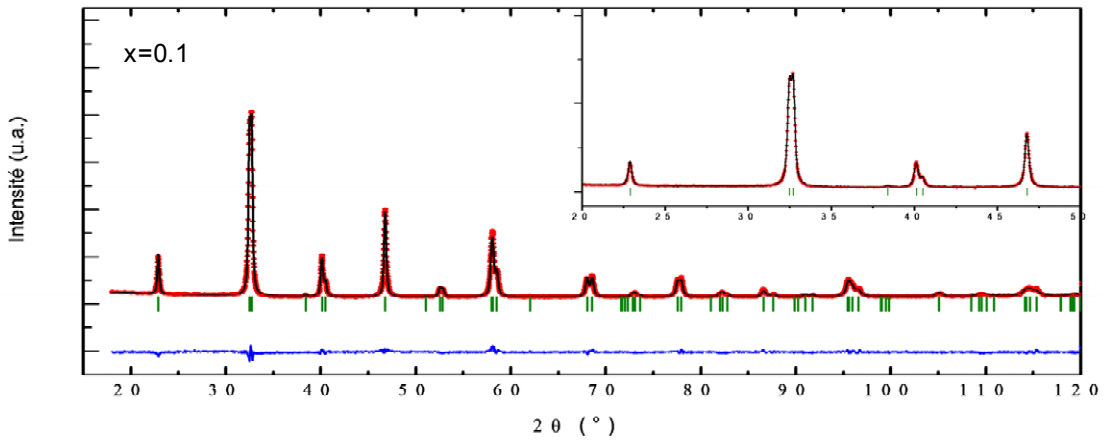

Figure S3 : Observed (red dots), calculated (black solid line), and difference (bottom, blue) X-ray powder diffraction patterns for $La_{1-x}Sr_xMnO_{3+\delta}$ with x = 0.1. A zoom in the 20-50° theta range is presented in the inset.

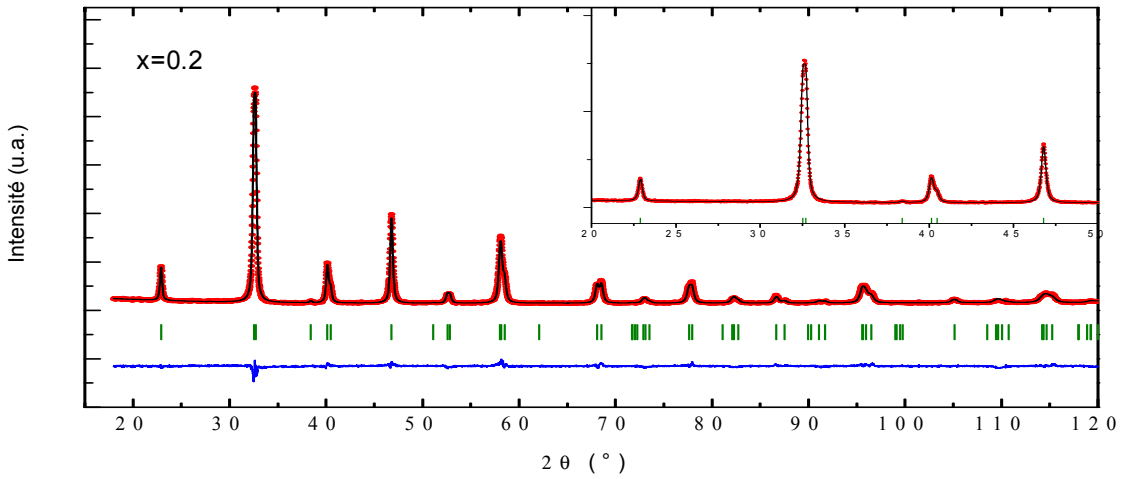

Figure S4 : Observed (red dots), calculated (black solid line), and difference (bottom, blue) X-ray powder diffraction patterns for $La_{1-x}Sr_xMnO_{3+\delta}$ with x = 0.2. A zoom in the 20-50° theta range is presented in the inset.

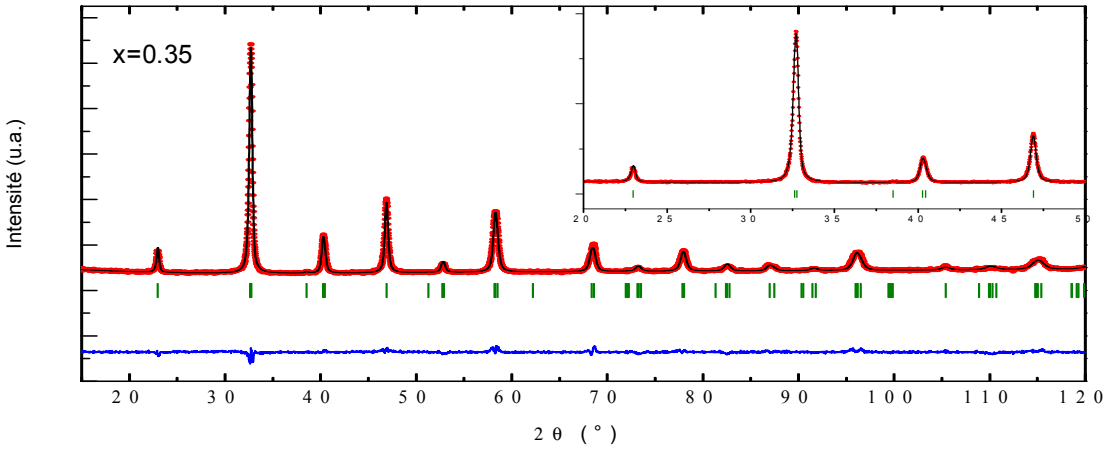

Figure S5 : Observed (red dots), calculated (black solid line), and difference (bottom, blue) X-ray powder diffraction patterns for $La_{1-x}Sr_xMnO_{3+\delta}$ with x = 0.35. A zoom in the 20-50° theta range is presented in the inset.

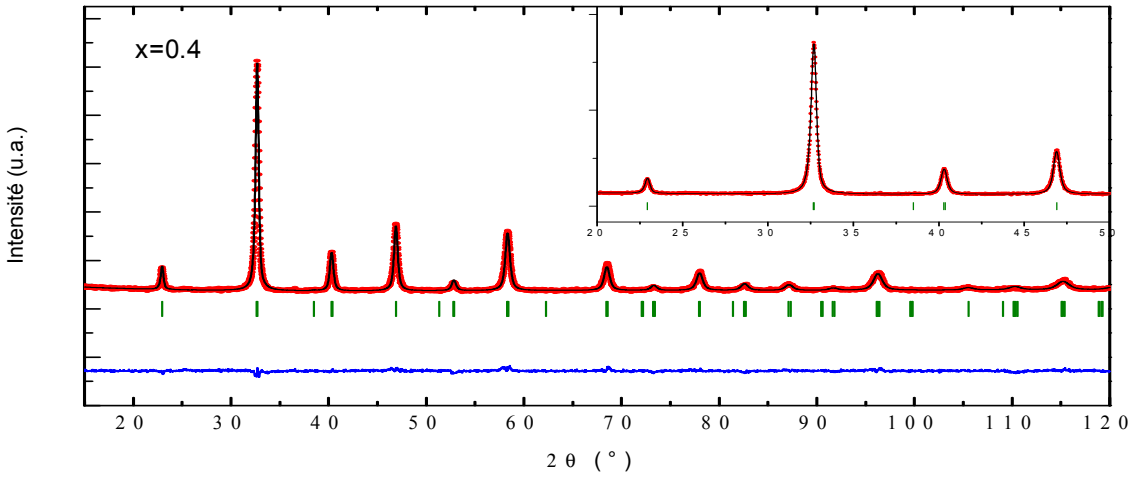

Figure S6 : Observed (red dots), calculated (black solid line), and difference (bottom, blue) X-ray powder diffraction patterns for $La_{1-x}Sr_xMnO_{3+\delta}$ with x = 0.4. A zoom in the 20-50° theta range is presented in the inset.

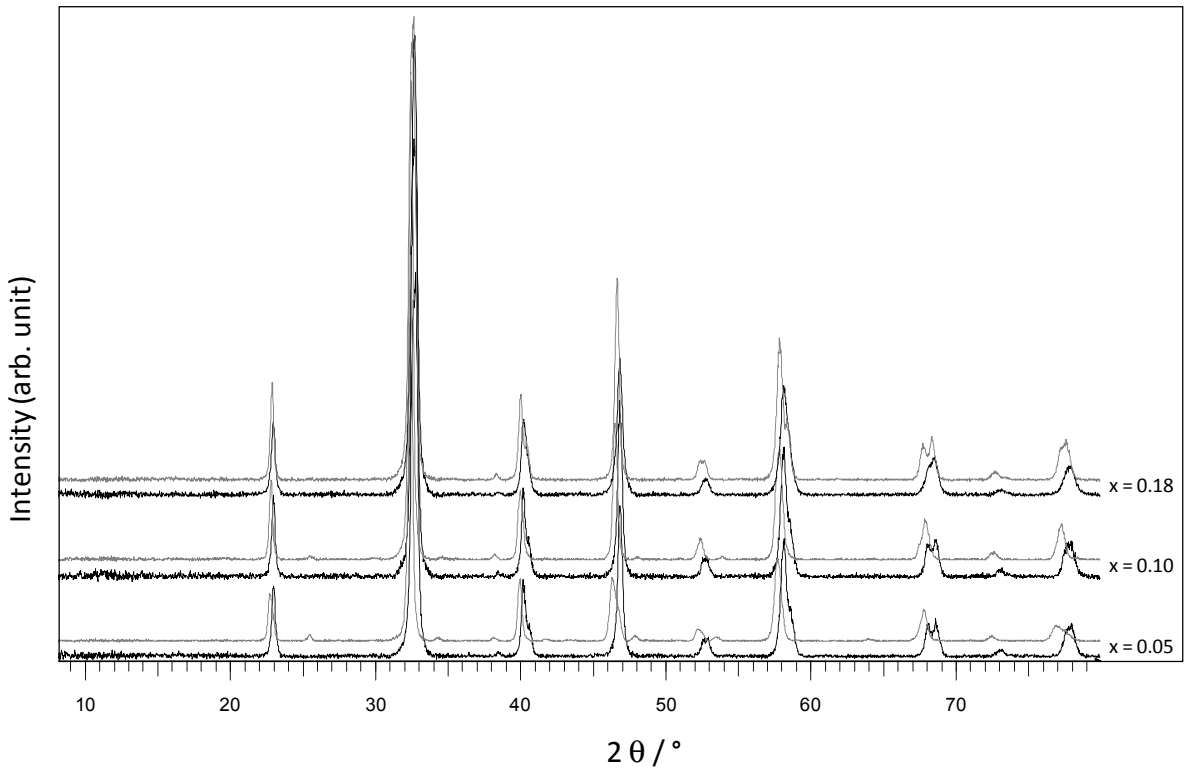

Figure S7 : XRD patterns of raw (grey) and reduced (black) $La_{1-x}Sr_xMnO_{3+\delta}$ samples with x equal to 0.05, 0.10 and 0.18.